ORIGINAL ARTICLE

Macrocyclic chelator-coupled gastrin-based radiopharmaceuticals for targeting of gastrin receptor-expressing tumours

Stephan Good · Martin A. Walter · Beatrice Waser ·
Xuejuan Wang · Jan Müller-Brand · Martin P. Béhé ·
Jean-Claude Reubi · Helmut R. Maecke

Abstract

Purpose Diethylenetriamine-pentaacetic acid (DTPA)-coupled minigastrins are unsuitable for therapeutic application with the available β-emitting radiometals due to low complex stability. Low tumour-to-kidney ratio of the known radiopharmaceuticals is further limiting their potency. We used macrocyclic chelators for coupling to increase complex stability, modified the peptide sequence to enhance radiolytic stability and studied tumour-to-kidney ratio and metabolic stability using ^{111}In-labelled derivatives.

Methods Gastrin derivatives with decreasing numbers of glutamic acids were synthesised using ^{111}In as surrogate for therapeutic radiometals for in vitro and in vivo studies. Gastrin receptor affinities of the ^{nat}In-metallated compounds were determined by receptor autoradiography using ^{125}I-

CCK as radioligand. Internalisation was evaluated in AR4-2J cells. Enzymatic stability was determined by incubating the ^{111}In-labelled peptides in human serum. Biodistribution was performed in AR4-2J-bearing Lewis rats.

Results IC_{50} values of the ^{nat}In-metallated gastrin derivatives vary between 1.2 and 4.8 nmol/L for all methionine-containing derivatives. Replacement of methionine by norleucine, isoleucine, methionine-sulfoxide and methionine-sulfone resulted in significant decrease of receptor affinity (IC_{50} between 9.9 and 1,195 nmol/L). All cholecystokinin receptor affinities were >100 nmol/L. All ^{111}In-labelled radiopeptides showed receptor-specific internalisation. Serum mean-life times varied between 2.0 and 72.6 h, positively correlating with the number of Glu residues. All ^{111}In-labelled macrocyclic chelator conjugates showed higher tumour-to-kidney ratios after 24 h (0.37–0.99) compared to ^{111}In-DTPA-minigastrin 0 (0.05). Tumour wash out between 4 and 24 h was low. Imaging studies confirmed receptor-specific blocking of the tumour uptake.

Conclusions Reducing the number of glutamates increased tumour-to-kidney ratio but resulted in lower metabolic stability. The properties of the macrocyclic chelator-bearing derivatives make them potentially suitable for clinical purposes.

Keywords Cholecystokinin · Gastrin · Minigastrin · Macrocyclic chelator · Medullary thyroid carcinoma

SG and MAW contributed equally to this work.

S. Good · X. Wang · H. R. Maecke (✉)
Division of Radiological Chemistry, University Hospital Basel,
Petersgraben 4,
4031 Basel, Switzerland
e-mail: hmaecke@uhbs.ch

M. A. Walter · J. Müller-Brand
Institute of Nuclear Medicine, University Hospital,
Basel, Switzerland

M. P. Béhé
Department of Nuclear Medicine, Philipps-University of Marburg,
Marburg, Germany

B. Waser · J.-C. Reubi
Department of Pathology, University of Berne,
Bern, Switzerland

Introduction

Gastrin is a 34-, 17- or 14-amino-acids-containing peptide that regulates acid secretion and proliferation of the gastric mucosa [1]. It is synthesised in the gastric G cells as a preprohormone and is post-translationally cleaved to form a family of

peptides with identical carboxytermini [2]. Gastrin binds to the cholecystokinin (CCK) receptors, which are found physiologically on parietal and enterochromaffin-like cells.

The two receptors of the gastrin-CCK family that consists of the CCK and the gastrin receptor are G-protein-coupled receptors [3]. Gastrin shows low affinity to the CCK receptor, which is mainly expressed in the gall bladder, gastric smooth muscle, pancreas and peripheral nerve system. Conversely, gastrin has high affinity to the gastrin receptor, which is mainly expressed in the gastric mucosa, endocrine pancreas and brain [4, 5]. Gastrin receptors are also overexpressed in medullary thyroid cancer [6], small cell lung cancer, stromal ovarian cancer, gastrointestinal adenocarcinoma and in neuroendocrine tumours [7–10]. Therefore, the gastrin receptor appears to be a promising target for diagnostic and therapeutic application of radiolabelled gastrin analogues [11–14].

Non-sulfated CCK analogues or, alternatively, minigastrin analogues, have recently been introduced for imaging and treatment of medullary thyroid carcinoma patients [15–22]. Derivatives for labelling with ^{111}In or ^{90}Y employed the acyclic chelator diethylenetriamine-pentaacetic acid (DTPA); however, the [^{90}Y-DTPA] monoamide complexes are not stable enough for targeted radionuclide therapy [23]. To increase the complex stability, a DTPAGlu chelator was employed [21]; however, the low tumour-to-kidney ratio restricted its therapeutic use [18, 19, 22]. Alternatively, macrocyclic chelators like 1,4,7,10-tetraazacyclododecane-1,4,7,10-tetraacetic acid (DOTA) or 1-(1-carboxy-3-carboxy-propyl)-1,4,7,10-tetraazacyclododecane-4,7,10-triacetic acid (DOTAGA) provide higher stability compared to acyclic chelators [24], whereas DOTAGA provides faster labelling kinetics [25, 26].

Thus, we coupled minigastrins with macrocyclic chelators to increase their complex stability. We also modified the peptide sequence to increase the important tumour-to-kidney ratio and radiolytic stability.

Materials and methods

Synthesis of chelator–peptide conjugates

All chemicals were commercially available and used without further purification. DOTAGA(tBu)$_4$ and DOTA (tBu)$_3$ were synthesised as previously described [24, 27]. DTPA(tBu)$_3$ was obtained commercially (Mallinckrodt Medical, USA). All peptides were assembled on Rink amide MBHA resin (0.6 mmol/g; NovaBiochem, Switzerland) using solid phase peptide synthesis on a semiautomatic peptide synthesiser (Rink Combichem Technologies, Switzerland). Three equivalents of Fmoc-protected amino acids (NovaBiochem, Switzerland) based on resin loading

with 3.3 equivalents of N-hydroxy-benzotriazole, 3.3 equivalents of N,N'-diisopropylcarbodiimide and five equivalents of N-ethyldiisopropylamine were used for coupling (reaction time: 45 min). Fmoc was removed with 20% piperidine/N,N-dimethylformamide. The tBu-protected chelator was attached using two equivalents of the prochelator with two equivalents of O-(7-azabenzotriazol-1-yl)-1,1,3,3-tetramethyluronium hexafluoro-phosphate. Deprotection and cleavage from resin was performed by adding a solution of 91% of trifluoroacetic acid (TFA), 3% H$_2$O, 5% thioanisole and 1% of triisopropyl-silane. The crude product was precipitated using a 1:1 mixture of diisopropylether/petroletether. Purification was done by preparative high-performance liquid chromatography (HPLC) using Uptisphere UP5ODB/25M column (Laubscher Labs, Switzerland), Bischof 2250 HPLC pumps and λ-1010 UV-detector (Metrohm AG, Switzerland). The products were lyophilised and characterised by ESI-MS (Waters ZMD; Waters-Micromass, USA, with HP1100 Quaternary LC pump; Hewlett Packard, USA) or MALDI-MS (Voyager sSTR equipped with Nd/YAG laser (355 nm); Applied BioSystems, USA). Purity was checked by HPLC (Macherey-Nagel Nucleosil 120-3 C$_{18}$ reversed phase column on 1050 HPLC system; Hewlett Packard, Germany, Berthold LB506 Cl γ-detector, Germany) with the gradient: eluent A: 0.1% TFA in water, eluent B: acetonitrile; 0 min 95% A, 30 min 55% A, 32 min 0% A, 34 min 0% A; flow: 0.75 mL/min; λ: 214 nm.

Radiolabelling

Radiolabelling was performed as previously described [28]. Three hundred microlitres of a 0.4 mol/L sodium acetate buffer pH 5 was added to an aliquot of 5 μg of the corresponding peptide–chelator conjugate, followed by 37 MBq [111]InCl$_3$ (Mallinckrodt, The Netherlands) and heated for 30 min at 95°C. For internalisation and serum stability studies, five equivalents of [nat]InCl$_3$ were added and heated again for 30 min to 95°C, and excess [nat]InCl$_3$ was separated by solid phase extraction using a SepPak C$_{18}$ cartridge (Waters, Switzerland). The radiopeptide was immobilised on the cartridge; excess of [nat]InCl$_3$ was rinsed off with water. Finally, the product was eluted with methanol, evaporated to dryness and reconstituted in water. Quality control after radiolabelling was performed using the HPLC system described above and the following gradient: eluent A: 0.1% TFA in water, eluent B: acetonitrile; 0 min 95% A, 5 min 95% A, 10 min 0% A, 15 min 0% A; flow: 0.75 mL/min.

Binding affinity studies on CCK- or gastrin-expressing tissues

Binding affinities were evaluated as previously described [29] in surgically extracted human tumour tissues selected

from previous experiments to express either cholecystokinin and gastrin receptors [5, 7]. Increasing amounts of ^{nat}In-labelled minigastrin derivatives were added to the ^{125}I-labelled D-Tyr-Gly-Asp-Tyr(SO$_3$H)-Nle-Gly-Trp-Nle-Asp-Phe-amide (^{125}I-CCK) containing incubation medium to generate competitive inhibition curves. Tissue slides were exposed to Biomax MR films (Kodak) for 1–7 days. Autoradiograms were quantified using tissue standards for iodinated compounds (Amersham, UK) [30].

Enzymatic stability in human serum

After labelling with ^{111}In/^{nat}InCl$_3$, 40 pmol of each compound was added to 2 mL fresh human blood serum and incubated at 37°C and 5% CO$_2$; 150 μL of this solution was removed at different time intervals and added to 150 μL of ethanol. The precipitate was separated by centrifugation (10 min, 1,850×g, 4°C). The supernatant was analysed by HPLC as described above.

Cell culture and in vitro internalisation assay on AR4-2J cells

Gastrin receptor-positive AR4-2J rat pancreatic tumour cells [31] were kept in Dulbecco's Modified Eagle Medium (DMEM) supplemented with 10% fetal bovine serum, amino acids and vitamins (Amimed, BioConcept, Switzerland). The internalisation experiments were performed as previously described [32, 33]. One million AR4-2J cells were washed with DMEM and allowed to rest for 1 h at 37°C in 1.2 mL of medium. An amount of 0.25 pmol (2.8 kBq) of the ^{111}In/^{nat}In-labelled chelator–peptide conjugates was added to a final concentration of 0.167 nmol/L, and cells were incubated at 37°C in 5% CO$_2$. To study non-receptor-specific uptake, >10^4-fold excess of unlabelled DOTA-minigastrin 11 (3 nmol/well) was added. The internalisation was stopped after different incubation times (30 min, 1, 2 and 4 h) by removal of the medium. Cells were washed twice with phosphate-buffered saline (pH 7.2, 4°C) and then twice with glycine buffer (5 min, 0.05 mol/L glycine, pH 2.8, 4°C) to discriminate between cell surface-bound (acid releasable) and internalised radioligand. Cells were then incubated with 1 mol/L NaOH (10 min, 37°C) to release them from the plate. All fractions were collected in triplicates, and quantitative γ-counting was done using a COBRA II, D 5003 γ-system well counter (Canberra Packard, USA).

Biodistribution and SPECT/CT imaging in AR4-2J-bearing Lewis rats

All animal experiments were approved and performed according to the national regulations for animal treatment (Bundesamt für Veterinärwesen, approval no. 789). Ten

million AR4-2J rat pancreatic tumour cells were subcutaneously implanted in the right posterior limb of 6-week-old Lewis rats (Harlan, The Netherlands). Two weeks after inoculation of the tumour cells, 0.1 nmol (1.1 MBq) of the corresponding ^{111}In-labelled chelator–peptide conjugate (dissolved in 200 μL of saline supplemented with 0.1% human serum albumin) was injected intravenously under inhalation anaesthesia (3 vol.% isoflurane with 0.6 L O$_2$/min). To determine non-specific tumour uptake, 100 μg (71.3 nmol) unlabelled DOTA-minigastrin 11 was added to the injection solution. The rats (in groups of three to five animals, 160–180 g body weight and 6–15 mm tumour diameter) were sacrificed 4 or 24 h post-injection, respectively, under anaesthesia.

Organs of interest were collected, rinsed of excess blood, plotted dry and weighed. The radioactivity of the different samples was quantified on a γ-counter.

Four hours after injection of the radioligand, the sacrificed animals were placed on a SPECT/CT-camera (Symbia T2, Siemens, Germany) for the acquisition of images. Iteratively reconstructed SPECT images (four subsets, eight iterations) were combined with three-dimensional reconstructed images from the spiral CT (1.25 mm slices, 1.2 mm reconstruction increment, 130 kV, 48 mA s).

Statistical methods

Discrete variables are expressed as counts (percentage) and continuous variables as mean ± standard deviation, unless stated otherwise. A first-order decay model was used to calculate serum mean-life time values. Receptor-specific internalisation was calculated as difference between non-blocked and blocked uptake and expressed as percentage of applied activity. Organ uptakes were calculated and expressed as percentage of injected activity per gram tissue (%IA/g). A linear regression model was employed to examine the association of internalisation rates, binding affinities, tumour uptake and kidney uptake. p values of <0.05 were considered to be statistically significant.

Results

Synthesis of chelator–peptide conjugates

The following compounds were synthesised: DOTA-minigastrin 9 (minigastrin 9: DGlu-Glu-Glu-Ala-Tyr-Gly-Trp-Met-Asp-Phe-NH$_2$), DOTA-minigastrin 10 (minigastrin 10: DGlu-Glu-Ala-Tyr-Gly-Trp-Met-Asp-Phe-NH$_2$), DOTA-minigastrin 11 (minigastrin 11: DGlu-Ala-Tyr-Gly-Trp-Met-Asp-Phe-NH$_2$), DOTAGA-minigastrin 11 and DTPA-minigastrin 11 (Fig. 1). In addition, DOTA-minigastrin 11-based compounds, with the amino acid methionine replaced by
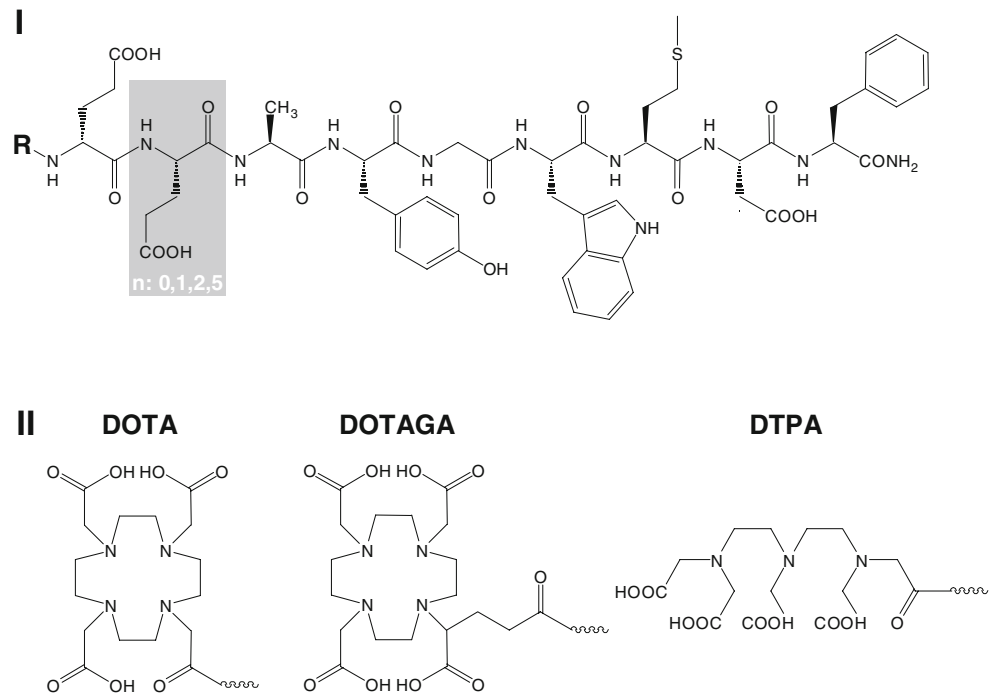
isoleucine (Ile), norleucine (Nle), methionine-sulfoxide (Met (O)) or methionine-sulfone (Met(O$_2$)) were synthesised. All conjugates showed purities >95% as confirmed by HPLC; identities were confirmed by mass spectroscopy. Both synthesised DTPA-conjugates showed shorter HPLC retention times than the DOTA-conjugates (Table 1).

Radiolabelling with ^{111}InCl$_3$

Radiolabelling of all chelator–peptide conjugates with ^{111}In and quality control using HPLC resulted in the following retention times and radiochemical purities: [^{111}In-DTPA]-

minigastrin 0 (retention time: 21.82 min; radiochemical purity: 99.0%); [^{111}In-DTPA]-minigastrin 11 (22.30 min; 99.9%); [^{111}In-DOTA]-minigastrin 9 (22.90 min; 95.9%); [^{111}In-DOTA]-minigastrin 10 (22.97 min; 97.8%); [^{111}In-DOTA]-minigastrin 11 (22.90 min; 97.5%); [^{111}In-DOTAGA]-minigastrin 11 (22.85 min; 99.4%).

Binding affinity studies on CCK-positive tissues

Receptor binding affinities to cholecystokinin and gastrin receptor-positive tumour cells are expressed as IC$_{50}$ values, describing the concentration of the tested substance needed

Table 1 Mass spectrometry and HPLC data of the studied minigastrins

Compound	Calculated mass (g/mol)	Observed mass[a]	Purity[b] (%)	Retention time[c] (min)
DOTAGA-minigastrin 11	1,474.6	1,475.6, [M+H]$^+$; 85% 1,497.3, [M+Na]$^+$; 100% 1,519.6, [M+2 Na–H]$^+$; 46%	97.3	27.88
DOTA-minigastrin 11	1,402.6	1,403.6, [M+H]$^+$; 100% 1,425.4, [M+Na]$^+$; 55% 1,441.3, [M+2 Na–H]$^+$; 30%	98.2	27.85
DOTA-minigastrin 10	1,531.6	1,532.4, [M+H]$^+$; 100% 1,554.5, [M+Na]$^+$; 25%	96.8	27.62
DOTA-minigastrin 9	1,660.7	1,661.5, [M+H]$^+$; 100% 1,683.5, [M+Na]$^+$; 25%	97.8	27.47
DTPA-minigastrin 11	1,391.5	1,392.4, [M+H]$^+$; 18% 1,414.4, [M+Na]$^+$; 100% 1,436.3, [M+2 Na]$^+$; 38%	96.3	26.84
DTPA-minigastrin 0	2,036.8	2,059.3, [M+Na]$^+$; 100% 2,075.2, [M+K]$^+$; 55%	95.8	26.63

[a] Assessed by mass spectrometry, mass in grams per mole, interpretation, relative abundance
[b] Evaluated by HPLC (gradient I)

Table 2 Gastrin and cholecystokinin receptor binding affinities of the studied minigastrins

Compound	n	Binding affinity to the gastrin receptor	Binding affinity to the cholecystokinin receptor
[DTPA]- minigastrin 0	6	0.98±0.4	>100
[In-DOTA]-minigastrin 9	2	1.2±0.4	>100
[In-DOTA]-minigastrin 10	2	2.5±0.1	>100
[In-DOTA]-minigastrin 11	6	4.8±0.7	>100
[In-DOTAGA]-minigastrin 11	2	3.4±2.0	>100
[In-DTPA]-minigastrin 11	3	3.9±0.6	–
[In-DOTA]-DGlu-Ala-Tyr-Gly-Trp-Nle[15]-Asp-Phe-NH$_2$	2	9.9±0.1	>1,000
[In-DOTA]-DGlu-Ala-Tyr-Gly-Trp-Ile[15]-Asp-Phe-NH$_2$	2	200±5.0	>1,000
[In-DOTA]-DGlu-Ala-Tyr-Gly-Trp-Met(O$_2$)[15]-Asp-Phe-NH$_2$	2	1,195±760	>1,000
[In-DOTA]-DGlu-Ala-Tyr-Gly-Trp-Met(O)[15]-Asp-Phe-NH$_2$	2	1,096±116	>1,000

Binding affinities are expressed as IC$_{50}$ values (nanomoles per litre) in mean ± SD
n Number of experiments

to inhibit the binding of ^{125}I-CCK by 50%. These IC$_{50}$ values are listed in Table 2. All compounds having the native seven carboxyterminal amino acids showed IC$_{50}$ values <5 nmol/L to the gastrin receptor and IC$_{50}$ values >100 nmol/L to the cholecystokinin receptor. IC$_{50}$ values to the gastrin receptor were reduced when the amino acid methionine was replaced by norleucine (factor 2), isoleucine (factor 42), methionine-sulfone and methionine-sulfoxide (both factor >200).

Enzymatic stability in human blood serum

Time-dependent degradation of the minigastrin analogues are presented in Fig. 2. The corresponding mean-life times

Fig. 2 Serum stabilities of the ^{111}In-labelled minigastrins: *filled squares* [^{111}In-DTPA]-minigastrin 0, *grey triangles* [^{111}In-DOTA]-minigastrin 9, *inverted grey triangles* [^{111}In-DOTA]-minigastrin 10, *plus signs* = [^{111}In-DOTAGA]-minigastrin 11, *grey circles* [^{111}In-DTPA]-minigastrin 11, *filled diamonds* [^{111}In-DOTA]-minigastrin 11, *ex marks* [^{111}In-DOTA, Nle[15]]-minigastrin 11
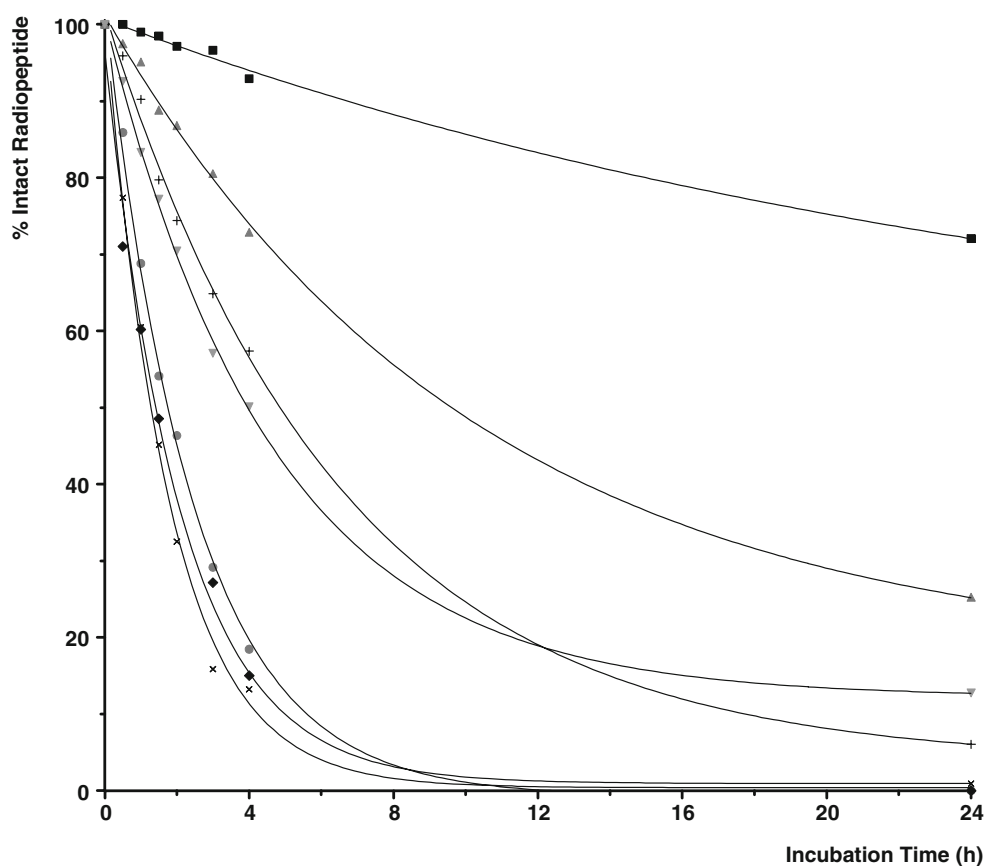
Table 3 Internalisation rates after 4-h incubation

Compound	Internalisation rate	n	p^a
[^{111}In-DTPA]-minigastrin 0	14.1±0.6%	3	–
[^{111}In-DOTA]-minigastrin 9	11.0±2.3%	12	0.002
[^{111}In-DOTA]-minigastrin 10	6.4±1.0%	9	0.000
[^{111}In-DOTA]-minigastrin 11	10.4±0.8%	9	0.001
[^{111}In-DOTAGA]-minigastrin 11	9.7±3.1%	12	0.001
[^{111}In-DTPA]-minigastrin 11	8.9±1.2%	9	0.000
[^{111}In-DOTA]-[Nle^{15}]-minigastrin 11	7.5±0.5%	3	0.009

Internalisation rates are expressed in percentage of injected activity per million cells in mean ± SD

n Number of experiments

^{a} p vs. [^{111}In-DTPA]-minigastrin 0

of the radiolabelled compounds in human blood serum were as follows: [^{111}In-DTPA]-minigastrin 0 (72.6 h), [^{111}In-DOTA]-minigastrin 9 (15.4 h), [^{111}In-DOTAGA]-minigastrin 11 (7.2 h), [^{111}In-DOTA]-minigastrin 10 (5.8 h), [^{111}In-DTPA]-minigastrin 11 (2.6 h), [^{111}In-DOTA]-minigastrin 11 (2.4 h), [^{111}In-DOTA, Nle^{15}]-minigastrin 11 (2.0 h).

In vitro internalisation into AR4-2J cells

The internalised fractions, expressed as percent of the injected activity per 1 million cells over a 4-h period, are shown in Table 3. The 4-h values of all compounds significantly decreased to <0.5% after addition of excess of

unlabelled DOTA-minigastrin 11 ($p<0.001$). The surface-bound radioligand did not exceed 2% of the added radioactivity after 4 h.

Biodistribution studies in AR4-2J-bearing Lewis rats

Organ uptakes are listed in Table 4; a detailed list is provided in Supplemental Table 1. [^{111}In-DTPA]-minigastrin 0 (0.64± 0.11% I.A./g) and [^{111}In-DOTA]-minigastrin 9 (0.68± 0.40%) showed 4-h tumour uptake values distinctly higher compared to [^{111}In-DOTA]-minigastrin 10 (0.32±0.15%), [^{111}In-DOTA]-minigastrin 11 (0.31±0.04%) and [^{111}In-DOTAGA]-minigastrin 11 (0.34±0.09%). The difference in tumour uptake was not significant between [^{111}In-DOTA]-minigastrin 11 and [^{111}In-DOTAGA]-minigastrin 11 ($p= 0.71$). High tumour uptakes were found along with high binding affinities ($r=0.85$, Fig. 3a), high internalisation rates ($r=0.71$, Fig. 3b) and high blood serum stabilities ($r=0.67$, Fig. 3c). Coinjection of excess of unlabelled DOTA-mini-gastrin 11 significantly reduced the uptake of [^{111}In-DOTA]-minigastrin 11 into the tumour by 87% (Table 4) and of [^{111}In-DOTA]-minigastrin 9 by 84%. The uptake into the stomach was reduced by 84% for [^{111}In-DOTA]-minigastrin 11 and by 93% for [^{111}In-DOTA]-minigastrin 9. [^{111}In-DTPA]-minigastrin 0 showed the highest kidney uptake after 4 h (8.66±0.44%), followed by [^{111}In-DOTA]-minigastrin 9 (1.46±0.23%), [^{111}In-DOTA]-minigastrin 11 (0.36±0.07%), [^{111}In-DOTAGA]-minigastrin 11 (0.33±0.01%) and [^{111}In-DOTA]-minigastrin 10 (0.32±0.02%; Table 4). The kidney uptake was negatively correlated to the overall compound

Table 4 Biodistribution data of the studied minigastrins

Compound	Values	Tumour	Stomach	Pancreas	Kidney	Tumour/ kidney	Tumour/ stomach
[^{111}In-DTPA]-minigastrin 0	4 h ($n=5$)	0.64±0.11	0.16±0.01	0.01±0.00	8.66±0.44	0.07	3.88
	24 h ($n=2$)	0.58±0.22	0.18±0.00	0.03±0.02	10.5±4.11	0.05	3.25
[^{111}In-DOTA]-minigastrin 9	4 h ($n=5$)	0.68±0.40*	0.14±0.05	0.01±0.00	1.46±0.23**	0.46	11.1
	4 h blocked^a ($n=5$)	0.11±0.00***	0.01±0.00	0.00±0.00	1.13±0.13		
	24 h ($n=3$)	0.45±0.31	0.05±0.02	0.01±0.00	1.22±0.55	0.37	9.55
[^{111}In-DOTA]-minigastrin 10	4 h ($n=5$)	0.32±0.15**	0.06±0.01	0.01±0.01	0.32±0.02**	1.01	5.23
	24 h ($n=3$)	0.28±0.22	0.02±0.01	0.01±0.00	0.38±0.01	0.73	12.1
[^{111}In-DOTA]-minigastrin 11	4 h ($n=4$)	0.31±0.04**	0.05±0.01	0.01±0.00	0.36±0.07**	0.89	6.42
	4 h blocked^a ($n=5$)	0.04±0.01****	0.01±0.00	0.00±0.00	0.31±0.02		
	24 h ($n=3$)	0.34±0.01	0.02±0.01	0.01±0.00	0.34±0.04	0.99	14.8
[^{111}In-DOTAGA]-minigastrin 11	4 h ($n=4$)	0.34±0.09**	0.07±0.02	0.00±0.00	0.33±0.01**	1.02	4.98
	24 h ($n=3$)	0.28±0.19	0.05±0.01	0.00±0.00	0.40±0.06	0.71	6.20
[^{111}In-DOTA, Nle^{15}]-minigastrin 11	4 h ($n=3$)	0.80±0.43	0.07±0.02	0.01±0.01	0.35±0.03	2.25	12.3
	24 h ($n=3$)	0.24±0.16	0.01±0.01	0.00±0.00	0.35±0.07	0.70	20.0

Uptake as percentage of injected activity per gram tissue, mean value ± SD

n Number of tested animals

* $p=0.85$ vs. [^{111}In-DTPA]-minigastrin 0; ** $p<0.01$ vs. [^{111}In-DTPA]-minigastrin 0; *** $p=0.04$ vs. unblocked [^{111}In-DOTA]-minigastrin 9; **** $p<0.01$ vs. unblocked [^{111}In-DOTA]-minigastrin 11

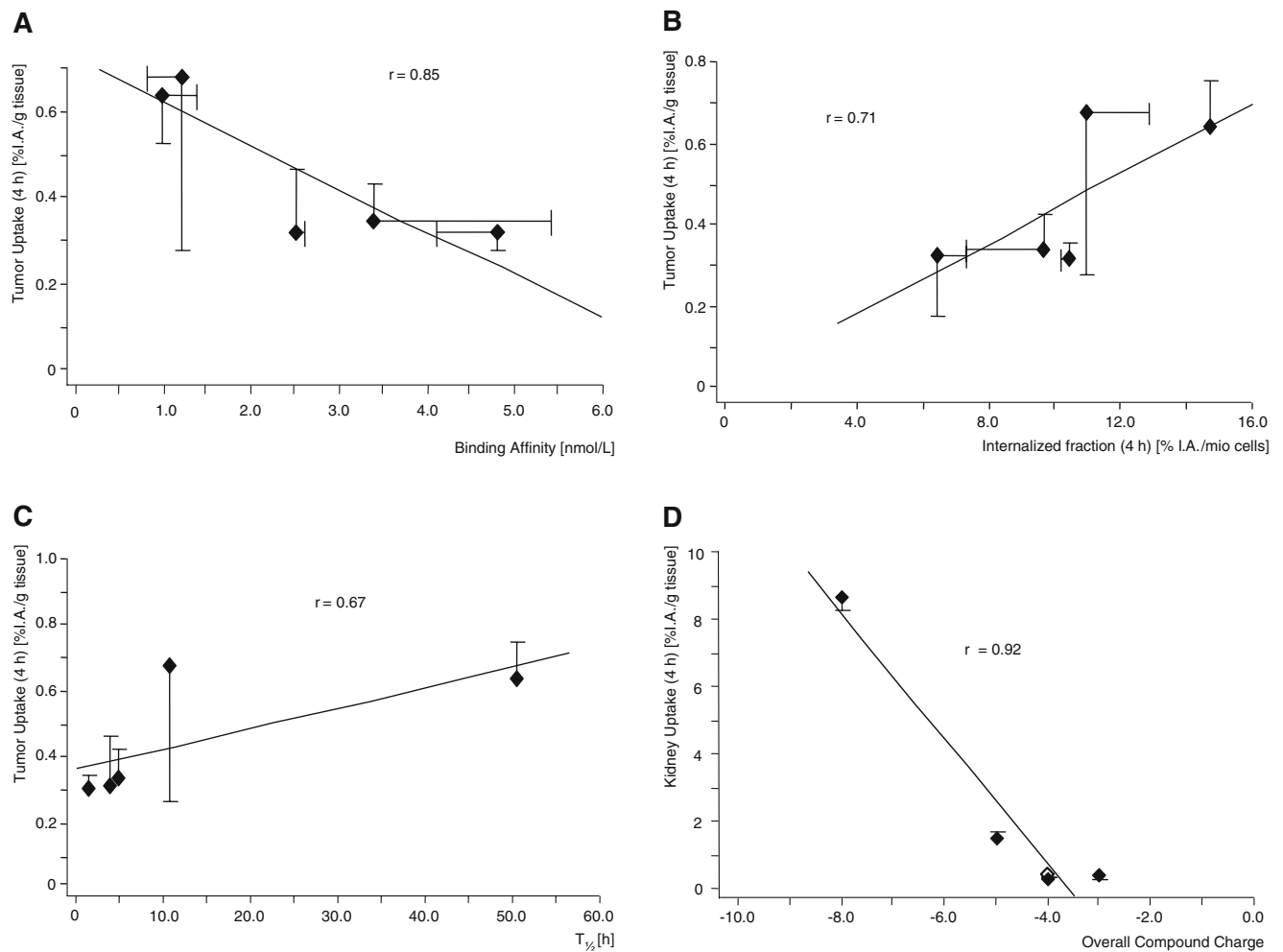^{a} Coinjection of 100 μg DOTA-minigastrin 11

Fig. 3 Correlation of binding affinity and tumour uptake (**a**), internalised fraction at 4 h and tumour uptake (**b**), serum stability and tumour uptake (**c**) and of overall charge and kidney uptake (**d**)

charge (r=0.96; Fig. 3d). Uptake in gastrin receptor-negative tissues, e.g. the kidneys, was not significantly influenced by excess of blocking agent (Table 4). The resulting tumour-to-kidney ratios 24 h post-injection were in the following, in increasing order (Table 4): [^{111}In-DTPA]-minigastrin 0 (0.05), [^{111}In-DOTA]-minigastrin 9 (0.37), [^{111}In-DOTA, Nle^{15}]-minigastrin 11 (0.70), [^{111}In-DOTAGA]-minigastrin 11 (0.71), [^{111}In-DOTA]-minigastrin 10 (0.73) and [^{111}In-DOTA]-minigastrin 11 (0.99). The 24-h tumour uptake

values were, except for [^{111}In-DOTA]-minigastrin 11, lower than the 4-h uptakes, but the decrease was not significant ($0.68 \geq p \geq 0.20$).

SPECT/CT imaging

The combined SPECT/CT image clearly showed the accumulation of the radiolabelled compounds in the tumour (Fig. 4).

Fig. 4 Coregistered SPECT/CT images of a Lewis rat bearing an AR4-2J tumour (**a**: *circle*) after application of 0.1 nmol (1.1 MBq) [^{111}In-DOTA]-minigastrin 11. Three-dimensional reconstruction using soft tissue (**a**) and skeletal (**b**) rendering
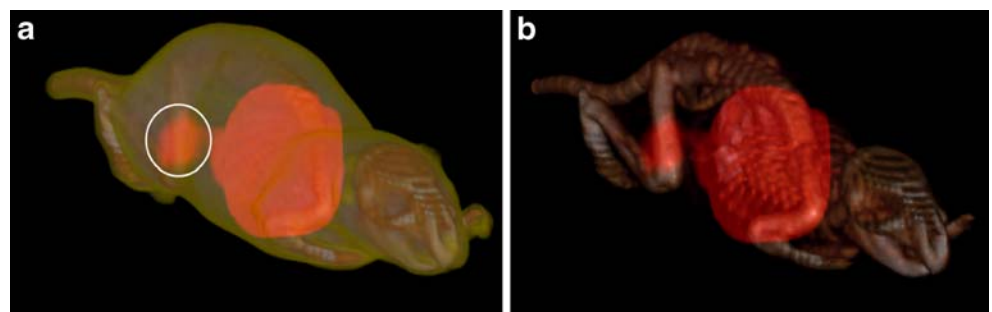
Discussion

DTPA-coupled minigastrin and CCK derivatives have previously been employed for labelling with radiometals [19, 21, 22]; however, the acyclic structure of DTPA led to a high rate of decomplexation of the radioisotopes. This instability restricted the therapeutic use of these radio-peptides [23]. Contrary to the acyclic chelator DTPA, the macrocyclic chelators DOTA and DOTAGA offer higher kinetic inertness and thereby prevent significant decom-plexation [34].

Coupling to macrocyclic chelators resulted in minigas-trin derivatives with the potential of a stable complexation of α- and β-emitting radiometals. Furthermore, decreasing the number of glutamic acid residues of the gastrin derivatives significantly increased the tumour-to-kidney ratio. These properties allow reduction of the undesired uptake of the radionuclide into non-target organs during radiopeptide therapy.

In this study, we successfully coupled both DOTA and DOTAGA to the gastrin derivatives, retaining a high binding affinity and receptor-specific internalisation capac-ity. The in vivo studies revealed low intestinal retention of our compounds, which indicates a low hepatobiliary excretion.

Methionine-containing radiopeptides like gastrin com-monly undergo auto-oxidation to sulfoxides during synthe-sis and more strikingly during radiolabelling. This effect is particularly observed after labelling with α- and β-emitting radionuclides, which frequently cause oxidation of thio-ether-containing amino acids via radiolysis [35]. On the one hand, this process can be suppressed by the addition of radical scavengers such as gentisic acid, ascorbic acid or methionine to the labelling solution [36]. On the other hand, the occurrence of auto-oxidation can be avoided by substitution of methionine with methionine mimics like methionine-sulfone, methionine-sulfoxide, norleucine or others [37]. However, in this study, replacement of methionine resulted in a distinct loss of binding affinity to the gastrin receptor, except for the norleucine derivative. This loss was considerable after employing isoleucine, methionine-sulfone or methionine-sulfoxide, respectively. Hence, these compounds, except the norleucine derivative, are unsuitable for receptor targeting.

Our results indicate that the number of negative charges of the N-terminally bound Glu residues in the sequence of minigastrin has a positive influence on metabolic stability and on binding affinity. We also used DOTAGA, among other reasons like fast labelling kinetics [25], to study if a chelate-based negative charge has a similar effect. The additional negative charge did also enhance the metabolic stability.

Kidney uptake of radiolabelled peptides by tubular reabsorption often restricts the maximum therapeutic dose [38] and, therefore, is the major limitation in radiopeptide therapy [39, 40]. Thus, reduction of kidney uptake is essential to improve the efficacy of radiopeptide therapy. On the one hand, coinjection of polyglutamic acid was shown to reduce the accumulation of DTPA-minigastrin 0 in the kidneys up to a factor of ten [41]; on the other hand, previous oral communications have indicated that modifi-cation of the peptides might also be useful to reduce kidney uptake [42, 43]. In our experiments, the modification of the peptide sequence even exceeded previously reported effects. Deletion of five glutamic acid residues in the sequence of minigastrin 0 led to a reduction of kidney accumulation by more than a factor of 25. This led to a subsequent improvement of tumour-to-kidney ratio despite the lower serum stability of the compounds. The lower tumour uptake must be ascribed to the lower metabolic stability. The decreased kidney uptake can potentially be explained by the loss of the negative charges of the glutamic acids, which may be responsible for tubular reabsorption of radiolabelled peptides. This hypothesis is strengthened by recent results from Behe et al. [41] of significantly reduced kidney uptake by coinjection of polyglutamates [41, 44]. If factors other than the overall compound charge also have affected renal retention, this may be shown with new series of gastrin-based peptides having different hydrophilic spacers. Interestingly, the use of the chelator DOTAGA did not increase the kidney uptake as compared to DOTA despite the additional negative charge. Among other factors, the low tumour uptake possibly is a result of the low gastrin receptor density on the AR4-2J cells. Notably, the reduction of the peptide sequence had only minor influence on the binding affinity. The slow wash out, as demonstrated by the insignificant decrease of tumour uptake after 24 h, may allow using the minigastrin derivatives for therapeutic applications. Furthermore, good imaging capabilities of gastrin-positive tissues were achieved, as shown by the SPECT/CT images of the AR4-2J tumour-bearing Lewis rat.

Our results have implications for further research directed towards a higher tumour uptake of the radio-labelled minigastrin analogues. We have shown that higher receptor affinity, as well as higher serum stability, results in higher tumour accumulation. Therefore, in upcoming studies, both factors have to be considered in order to achieve further progress in the development of radio-labelled minigastrin analogues.

[^{111}In-DOTA]-minigastrin 11 displayed the highest tumour-to-kidney ratio in the animal biodistribution studies. On the other hand, [^{111}In-DOTA]-minigastrin 9 showed the highest gastrin receptor affinity in human tissues, as well as the highest stability of the DOTA-coupled minigastrins in human blood serum. Which of the present compounds will

offer the greatest benefit to the patient, however, remains elusive to the first clinical trials.

In conclusion, our modified minigastrins show improved tumour-to-kidney ratios, while the coupling with DOTA and DOTAGA provides a high radiometal complex stability. These properties make these derivates favourable for clinical studies of gastrin receptor-positive tumours. Nevertheless, further developments leading to a higher metabolic stability should improve the bioavailability of the radiopharmaceutical.

References

1. Wank SA, Pisegna JR, de Weerth A. Cholecystokinin receptor family. Molecular cloning, structure, and functional expression in rat, guinea pig, and human. Ann N Y Acad Sci 1994;713:49–66.
2. Rehfeld JF. The endoproteolytic maturation of progastrin and procholecystokinin. J Mol Med 2006;84:544–50.
3. Noble F, Wank SA, Crawley JN, Bradwejn J, Seroogy KB, Hamon M, et al. International Union of Pharmacology. XXI. Structure, distribution, and functions of cholecystokinin receptors. Pharmacol Rev 1999;51:745–81.
4. Reubi JC. Peptide receptors as molecular targets for cancer diagnosis and therapy. Endocr Rev 2003;24:389–427.
5. Reubi JC, Waser B, Laderach U, Stettler C, Friess H, Halter F, et al. Localization of cholecystokinin A and cholecystokinin B-gastrin receptors in the human stomach. Gastroenterology 1997;112:1197–205.
6. Reubi J, Waser B. Unexpected high incidence of cholecystokinin B/gastrin receptors in human medullary thyroid carcinomas. Int J Cancer 1996;67:644–7.
7. Reubi JC, Schaer JC, Waser B. Cholecystokinin(CCK)-A and CCK-B/gastrin receptors in human tumors. Cancer Res 1997;57:1377–86.
8. Reubi JC, Waser B. Concomitant expression of several peptide receptors in neuroendocrine tumours: molecular basis for in vivo multireceptor tumour targeting. Eur J Nucl Med Mol Imaging 2003;30:781–93.
9. Gotthardt M, Behe MP, Beuter D, Battmann A, Bauhofer A, Schurrat T, et al. Improved tumour detection by gastrin receptor scintigraphy in patients with metastasised medullary thyroid carcinoma. Eur J Nucl Med Mol Imaging 2006;33:1273–9.
10. Gotthardt M, Behe MP, Grass J, Bauhofer A, Rinke A, Schipper ML, et al. Added value of gastrin receptor scintigraphy in comparison to somatostatin receptor scintigraphy in patients with carcinoids and other neuroendocrine tumours. Endocr Relat Cancer 2006;13:1203–11.
11. Behr TM, Jenner N, Radetzky S, Behe M, Gratz S, Yucekent S, et al. Targeting of cholecystokinin-B/gastrin receptors in vivo: preclinical and initial clinical evaluation of the diagnostic and therapeutic potential of radiolabelled gastrin. Eur J Nucl Med 1998;25:424–30.
12. de Jong M, Bakker W, Bernard B, Valkema R, Kwekkeboom D, Reubi J, et al. Preclinical and initial clinical evaluation of ^{111}In-labeled nonsulfated CCK8 analog: a peptide for CCK-B receptor targeted scintigraphy and radionuclide therapy. J Nucl Med 1999;40:2081–7.
13. Behr TM, Jenner N, Behe M, Angerstein C, Gratz S, Raue F, et al. Radiolabeled peptides for targeting cholecystokinin-B/gastrin receptor-expressing tumors. J Nucl Med 1999;40:1029–44.
14. Reubi JC. CCK receptors in human neuroendocrine tumors: clinical implications. Scand J Clin Lab Invest Suppl 2001; 234:101–4.
15. Kwekkeboom DJ, Bakker WH, Kooij PP, Erion J, Srinivasan A, de Jong M, et al. Cholecystokinin receptor imaging using an octapeptide DTPA-CCK analogue in patients with medullary thyroid carcinoma. Eur J Nucl Med 2000;27:1312–7.
16. Reubi JC, Maecke HR, Krenning EP. Candidates for peptide receptor radiotherapy today and in the future. J Nucl Med 2005;46:67S–75S.
17. von Guggenberg E, Behe M, Behr TM, Saurer M, Seppi T, Decristoforo C. ^{99m}Tc-labeling and in vitro and in vivo evaluation of HYNIC- and (Na-His)acetic acid-modified [D-Glu1]-minigastrin. Bioconjug Chem 2004;15:864–71.
18. Behe M, Becker W, Gotthardt M, Angerstein C, Behr TM. Improved kinetic stability of DTPA-DGlu as compared with conventional monofunctional DTPA in chelating indium and yttrium: preclinical and initial clinical evaluation of radiometal labelled minigastrin derivatives. Eur J Nucl Med Mol Imaging 2003;30:1140–6.
19. Behe M, Behr TM. Cholecystokinin-B (CCK-B)/gastrin receptor targeting peptides for staging and therapy of medullary thyroid cancer and other CCK-B receptor expressing malignancies. Biopolymers 2002;66:399–418.
20. Nock BA, Maina T, Behe M, Nikolopoulou A, Gotthardt M, Schmitt JS, et al. CCK-2/Gastrin receptor-targeted tumor imaging with ^{99m}Tc-labeled minigastrin analogs. J Nucl Med 2005;46:1727–36.
21. Aloj L, Caraco C, Panico M, Zannetti A, Del Vecchio S, Tesauro D, et al. In vitro and in vivo evaluation of ^{111}In-DTPAGlu-G-CCK8 for cholecystokinin-B receptor imaging. J Nucl Med 2004;45:485–94.
22. Behr TM, Behe MP. Cholecystokinin-B/Gastrin receptor-targeting peptides for staging and therapy of medullary thyroid cancer and other cholecystokinin-B receptor-expressing malignancies. Semin Nucl Med 2002;32:97–109.
23. Harrison A, Walker C, Parker D. The in vivo release of ^{90}Y from cyclic and acyclic ligand-antibody conjugates. Nucl Med & Biol 1991;18:469–76.
24. Eisenwiener KP, Powell P, Maecke HR. A convenient synthesis of novel bifunctional prochelators for coupling to bioactive peptides for radiometal labelling. Bioorg Med Chem Lett 2000;10:2133–5.
25. Good S, Maecke H. Kinetics of formation and dissociation of two DOTA-based chelator conjugates with ^{177}Lu. Eur J Nucl Med Mol Imaging 2003;30(Suppl 2):S319.
26. Good S, Maecke H. Stability and kinetics of formation of two macrocyclic chelator-conjugates. Nuklearmedizin 2004;43:A11.
27. Heppeler A, Froidevaux S, Mäcke HR, Jermann E, Béhé M, Powell P, et al. Radiometal-labelled macrocyclic chelator-derivatised somatostatin analogue with superb tumour-targeting properties and potential for receptor-mediated internal radiotherapy. Chemistry A European Journal 1999;5:1016–23.
28. Eisenwiener KP, Prata MI, Buschmann I, Zhang HW, Santos AC, Wenger S, et al. NODAGATOC, a new chelator-coupled somatostatin analogue labeled with [$^{67/68}$Ga] and [^{111}In] for SPECT, PET, and targeted therapeutic applications of somatostatin receptor (hsst2) expressing tumors. Bioconjug Chem 2002; 13:530–41.

29. Reubi J, Waser B, Schaer J, Laederach U, Erion J, Srinivasan A, et al. Unsulfated DTPA- and DOTA-CCK analogs as specific high-affinity ligands for CCK-B receptor-expressing human and rat tissues in vitro and in vivo. Eur J Nucl Med 1998;25:481–90.

30. Reubi JC, Kvols LK, Waser B, Nagorney DM, Heitz PU, Charboneau JW, et al. Detection of somatostatin receptors in surgical and percutaneous needle biopsy samples of carcinoids and islet cell carcinomas. Cancer Res 1990;50:5969–77.

31. Christophe J. Pancreatic tumoral cell line AR42J: an amphicrine model. Am J Physiol 1994;266:G963–G71.

32. Wild D, Schmitt JS, Ginj M, Maecke HR, Bernard BF, Krenning E, et al. DOTA-NOC, a high-affinity ligand of somatostatin receptor subtypes 2, 3 and 5 for labelling with various radio-metals. Eur J Nucl Med Mol Imaging 2003;30:1338–47.

33. Storch D, Behe M, Walter MA, Chen J, Powell P, Mikolajczak R, et al. Evaluation of [^{99m}Tc/EDDA/HYNIC^0]octreotide derivatives compared with [^{111}In-DOTA^0,Tyr^3, Thr^8]octreotide and [^{111}In-DTPA^0]octreotide: does tumor or pancreas uptake correlate with the rate of internalization? J Nucl Med 2005;46:1561–9.

34. Maecke H, Good S. Radiometals (non-Tc, non-Re) and bifunctional labeling chemistry. In: Vertes A, Nagy S, Klencsar Z, editors. Handbook of nuclear chemistry. Vol. 4. Netherlands; 2003, p. 279–314.

35. Bogni A, Bombardieri E, Iwata R, Cadini L, Pascali C. Stability of L-[S-methyl-^{11}C]methionine solutions. J Radioanal Nucl Chem 2003;256:199–203.

36. Liu S, Edwards DS. Stabilization of ^{90}Y-labeled DOTA-biomolecule conjugates using gentisic acid and ascorbic acid. Bioconjug Chem 2001;12:554–8.

37. Good S, Maecke H, Merlo A, Reubi JC. Development of NK-1 receptor mediated radiopharmaceuticals. Nuklearmedizin 2004;43: A7.

38. Breeman WA, de Jong M, Kwekkeboom DJ, Valkema R, Bakker WH, Kooij PP, et al. Somatostatin receptor-mediated imaging and therapy: basic science, current knowledge, limitations and future perspectives. Eur J Nucl Med 2001;28: 1421–9.

39. Trejtnar F, Laznicek M. Analysis of renal handling of radio-pharmaceuticals. Q J Nucl Med 2002;46:181–94.

40. de Jong M, Barone R, Krenning E, Bernard B, Melis M, Visser T, et al. Megalin is essential for renal proximal tubule reabsorption of ^{111}In-DTPA-octreotide. J Nucl Med 2005;46: 1696–700.

41. Behe M, Kluge G, Becker W, Gotthardt M, Behr TM. Use of polyglutamic acids to reduce uptake of radiometal-labeled minigastrin in the kidneys. J Nucl Med 2005;46:1012–5.

42. von Guggenberg E, Rupprich M, Virgolini I, Decristoforo C. ^{99m}Tc-HYNIC-Minigastrin: improved in vitro and in vivo properties of a short chain analogue. Eur J Nucl Med Mol Imaging 2005;32(Suppl 1):S35.

43. Behe M, Reubi JC, Nock B. Evaluation of a DOTA-minigastrin derivative for therapy and diagnosis for CCK-2 receptor positive tumours. Eur J Nucl Med Mol Imaging 2005;32(Suppl 1):S78.

44. Behr TM, Goldenberg DM, Becker W. Reducing the renal uptake of radiolabeled antibody fragments and peptides for diagnosis and therapy: present status, future prospects and limitations. Eur J Nucl Med 1998;25:201–12.